A Letters Journal Exploring the Frontiers of Physics

August 2007

EPL, **79** (2007) 30004
doi: 10.1209/0295-5075/79/30004

www.epljournal.org

Excitability of chaotic transients in a semiconductor laser

O. V. Ushakov[1], N. Korneyev[1], M. Radziunas[2], H. J. Wünsche[1] and F. Henneberger[1]

[1] *Institut für Physik, Humboldt-Universität zu Berlin - Newtonstr.15, 12489 Berlin, Germany*
[2] *Weierstraß-Institut für Angewandte Analysis und Stochastik - Mohrenstrasse 39, 10117 Berlin, Germany*

received 27 April 2007; accepted in final form 19 June 2007
published online 17 July 2007

PACS 05.45.-a – Nonlinear dynamics and chaos
PACS 42.55.Px – Semiconductor lasers; laser diodes
PACS 05.45.Jn – High-dimensional chaos

Abstract – Using a semiconductor laser with integrated optical feedback, excitability of high-dimensional chaotic transients is demonstrated in a continuous and autonomous system. The generic phase-space portrait behind our observation consists in a boundary crisis of a chaotic attractor with a saddle born in a saddle-node bifurcation of continuous-wave states. The excitation of the chaotic transients, performed by short optical pulses, exhibits a distinct threshold as well as a refractory time. The escape from the chaotic saddle is strictly single-exponential and the escape time is an inverse-power function of the the distance to the boundary crisis with —despite of high dimensionality— a critical exponent close to unity. The device is capable of emitting pulses with a delay that is more than two orders of magnitude longer than the time scale of the internal carrier-photon dynamics.

Two nonlinear dynamical phenomena treated so far only separately are combined in this letter: excitability and chaotic transients. Excitability means that the response of a system on external perturbations is "all" or "none" depending on whether the strength of the stimulus is above or below a critical threshold. Prominent examples of excitable systems are the spiking of neurons [1], the cardiac muscle [2], the dynamics of life populations [3], or nonlinear chemical reactions [4]. Recently, the excitability of optical systems has become a focus of interest [5–7]. Chaotic transients, on the other hand, are long episodes of chaotic behavior which end eventually at an attractor that is usually not chaotic. Such transients are generated by switching a control parameter across a boundary crisis through which a chaotic saddle (CS) is formed [8]. Chaotic transients have been studied mostly in nonautonomous systems, among them modulated CO_2 [9,10] and NMR [11] lasers and, theoretically, for semiconductor lasers under external injection [12].

Excitability requires a certain phase space configuration. An equilibrium state (or a small-amplitude orbit) is the only attractor available and serves as rest state. Close to it, a sharp separatrix between trajectories of different types must exist. One type of trajectories approaches the rest state directly and determines the subthreshold response. The trajectories beyond the separatrix undertake extended phase space excursions before returning and govern the superthreshold response. Such configurations appear generically after bifurcations where an extended periodic orbit is suddenly destructed [13]. Paradigmatic examples are the Canard transition in the FitzHugh-Nagumo model [2] and homoclinic bifurcations [6,14,15]. The ruin of the destructed orbit guides the long excursions after superthreshold stimulation in either case.

Our idea is to replace the regular orbit by a chaotic attractor (CA). Specifically, we consider the configuration sketched in fig. 1. A saddle-focus and a stable focus stemming from a nearby saddle-node (SN) bifurcation exist in close neighborhood. Branch u_2 of the unstable manifold of the saddle-focus goes to the stable focus representing the rest state. The other branch u_1 leads to a CS formed just before in a boundary crisis when a CA has touched the stable manifold of the same saddle-focus. Obviously, the stable manifold of the saddle-focus separates two completely different types of trajectories. Those below this separatrix are spiraling along unstable branch u_2 directly to the rest state. Those above follow unstable branch u_1 into the CS and reach the rest state only after moving for some time along the saddle. Accordingly, the perturbed system may exhibit two qualitatively different responses: immediate return to the rest state upon weak perturbations and a long chaotic excursion along the CS when the stimulus is strong enough to push the system beyond the separatrix.

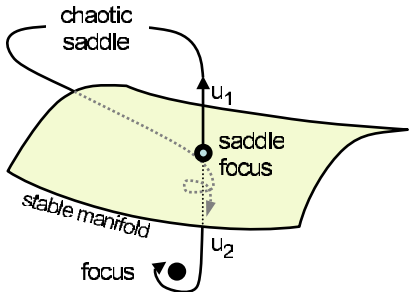

Fig. 1: Schematic phase-space portrait of an excitable chaotic saddle.

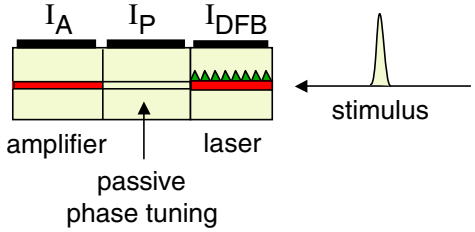

Fig. 2: Scheme of the multi-section semiconductor DFB laser with amplified optical feedback from the facet reflectivity $R \approx 30\%$. The injection currents are used to prepare the configuration of fig. 1. 30 ps optical pulses injected into the laser serve as stimuli.

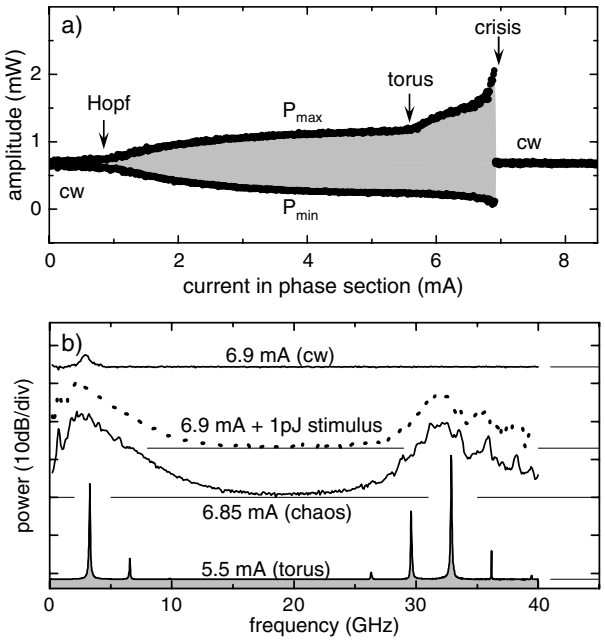

Fig. 3: Route of the multi-section laser into chaos. a) Maximum (P_{max}) and minimum (P_{min}) output power *vs.* phase current. The data are elaborated from time transients recorded with the sampling oscilloscope, $I_c = 6.87$ mA. b) Power spectra at selected phase currents belonging to the dynamics on the torus (5.5 mA), chaos (6.85 mA), and stationary cw state (6.9 mA). Dotted: Power spectrum at 6.9 mA under the superthreshold stimulation. Note the logarithmic scale and the power offset shown by thin horizontal lines. The other currents were $I_{DFB} = 41.7$ mA, $I_A = 49.5$ mA.

The phase-space configuration of fig. 1 is prepared by means of a multi-section semiconductor laser with integrated optical feedback. Such devices allow for the systematic realization of desired phase-space portraits by suitable choice of the injection currents [16]. Previously, excitability at a homoclinic bifurcation of a laser with passive feedback has been demonstrated [14]. The present laser structure, sketched in fig. 2, consists of a single-mode 1.55 μm distributed feedback (DFB) laser, a passive phase-tuning section made of a higher band-gap material, and a 1.55 μm amplifier section, all with the same length dimension of a few 100 μm. While the current I_{DFB} pumps the laser above threshold, I_A and I_P on the amplifier and passive section are to adjust strength and phase of the feedback, respectively. Details about the device are found in ref. [16]. The output is analyzed by a spectrum analyzer (bandwidth: 40 GHz) or, in order to record time transients, by a digital sampling oscilloscope (bandwidth: 50 GHz, sampling rate: 500 kHz). The external stimulus is represented by 30 ps long pulses generated with a commercial gain-switched semiconductor laser operating at 1.53 μm. The pulses with a maximum energy of 10 pJ and a repetition rate of 5 MHz are injected in the laser region of the multi-section device where they excite extra carriers markedly above the bandgap.

The control parameter of the present study is the phase current. Choosing I_{DFB} and I_A appropriately and tuning I_P, the device first changes to a self-pulsation mode, runs subsequently via a torus bifurcation into chaotic behavior, and, then, abruptly switches back at critical current I_c to continuous-wave (cw) operation. This is documented in figs. 3a and b where data extracted from time transients and power spectra are depicted, respectively. Motion on the torus is signified by two groups of sharp lines in the power spectrum. Here, relaxation and mode-beating oscillations coexist [16]. Chaotic behavior at larger phase currents is indicated by an extremely broad spectrum where the bimodal shape is reminiscent of the torus.

Locating the device relatively far above the critical current in the cw regime, the response on optical injection is indeed very similar to excitability (fig. 4). Relaxation oscillations and return to stable emission within about 2 ns are characteristics of small perturbations (panel a). Instead, for sufficiently large stimuli a distinct spike is generated followed by diffuse response (panel b). When plotting the height of the main spike versus the energy of the stimulation pulse, an "all-or-none" response with a sharp threshold is found (panel c).

Using pairs of stimulation pulses with tunable time-lag, the existence of a refractory period is evidenced (see [23]). The pulse pairs are generated by splitting the path of the optical injection in two branches of different length using 3 dB couplers as sketched on top of fig. 5. The shorter branch 1 contains a tunable delay line with an about 340 ps

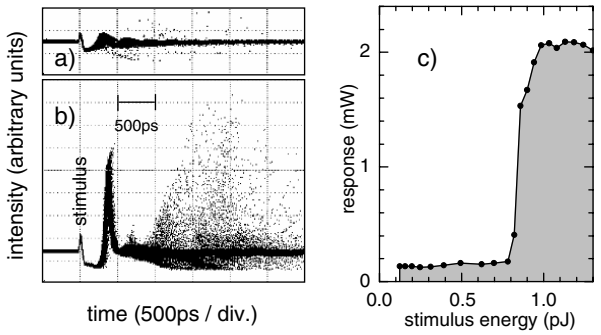

Fig. 4: Response of the multi-section laser on pulsed optical excitation ($I_P = 7.1\,\mathrm{mA}$). a) and b): Oscilloscope traces after sub- and superthreshold stimulation, respectively. Each panel collects hundreds of repeated excitations. c) Maximum device output *vs.* optical pulse energy.

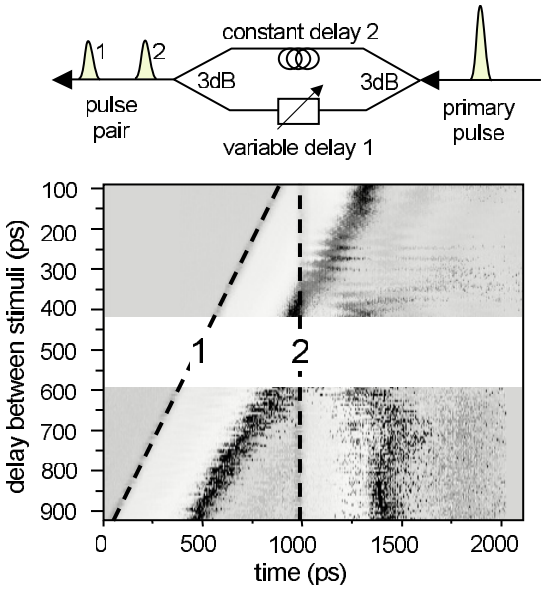

Fig. 5: Demonstration of refractory behavior ($I_P = 7.2\,\mathrm{mA}$). The pair of superthreshold stimuli 1 and 2 is marked by dashed lines in the plane (time, pulse-delay). The device response is grey coded (black: highest intensity, white: lowest intensity).

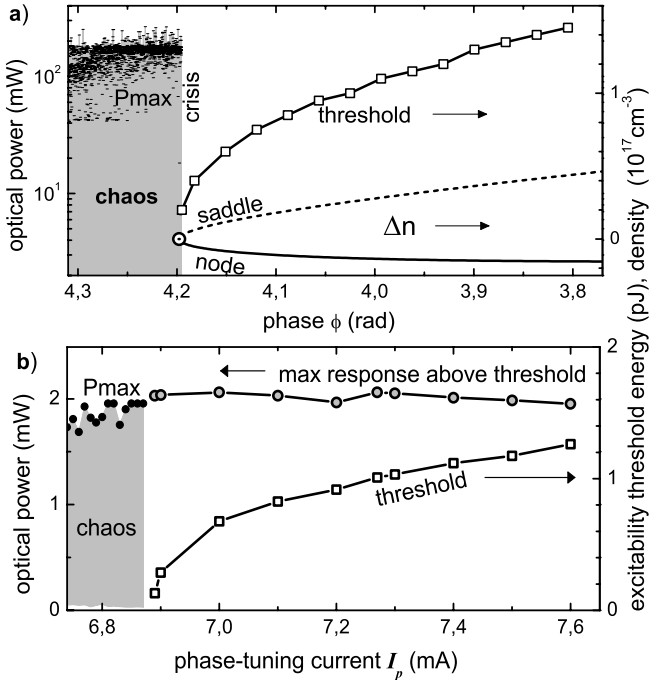

Fig. 6: Excitability threshold *vs.* distance from the boundary crisis. a) Calculation ($I_{DFB} = 40\,\mathrm{mA}$, $I_A = 28\,\mathrm{mA}$). SN bifurcation ($\odot$) and boundary crisis occur at feedback phase $\phi = 4.1936$ and $\phi_c = 4.1930$, respectively. Rectangles: stimulus energy at threshold, scattering dots left of ϕ_c: maximum device output in the chaotic regime computed over a time of 10 ns, lower solid and dashed lines: carrier inversion Δn on node and saddle, respectively, measured relative to its value at the SN bifurcation. b) Measurement ($I_{DFB} = 41.7\,\mathrm{mA}$, $I_A = 49.5\,\mathrm{mA}$). Meaning of rectangles and scattering dots as in a), circles: maximum spike strength under superthreshold stimulation (see [23]). Note that the power output right after the device edge is plotted in the calculation, while the experimental signal is attenuated by the various optical elements of the setup before detection.

continuous tuning range. Two fixed fiber lengths are used for path 2 resulting in accessible pulse-delay ranges of 90–430 ps and 590–930 ps, respectively. Both stimuli are well above threshold. For sufficiently long delays (lower part of the figure), the device responds by an individual spike upon each stimulus. However, when the second stimulus is injected too early, namely before the emission of the first spike, no extra reaction is observed. Exhibiting a sharp threshold as well a refractory period, the device response fulfills the main criteria of excitability. However, marked differences to the standard excitability scenario turn out, when the operation point is moved closer to the chaotic regime, as will be addressed below.

Numerical calculations based on the traveling-wave (TW) equations entirely confirm the experimentally observed pathway to chaos and reveal the underlying bifurcations. For a detailed description of the TW model as well as the parameter set, the reader is referred to our previous work [16]. In the calculations, instead of I_P, the feedback phase ϕ produced per round-trip in the passive section is directly used as control parameter. Figure 6 compares theoretical and experimental results. Note that increasing I_P means decreasing ϕ [16]. A SN bifurcation ($\odot$ in fig. 6a) occurs still within the chaotic domain. The resultant cw states are the stable focus and saddle-focus required in the phase-space portrait of fig. 1. Slightly right of the SN bifurcation at critical phase ϕ_c, the CA responsible for the chaotic behavior breaks up in a boundary crisis by touching the stable manifold of the saddle-focus. A close neighborhood of both transitions is achieved by proper choice of DFB and amplifier current.

The numerical analysis enables us to quantify the chaotic dynamics by computing the Lyapunov exponents. For this goal, the partial-differential TW equations are

approximated by ordinary differential equations (ODE) for a truncated set of optical modes [17]. The number of modes is carefully chosen to reproduce the solutions of the full TW model in the relevant ϕ range. Lyapunov exponents and Kaplan-Yorke dimension of the resulting 17 real ODE are calculated as described in ref. [18]. The Lyapunov spectra are nearly independent of ϕ within the grey-shaded interval of fig. 6a. In decreasing order, the first four exponents have approximate values of 2.7, 0, -1.0, and $-3.0\,\mathrm{ns}^{-1}$. The respective Kaplan-Yorke dimension varies between 3.3 and 3.7 and is thus indicative of a high-dimensional CA[1].

A distinct finding, both in experiment and theory, is that the stimulation threshold strongly declines when the device is set closer to the boundary crisis, whereas the strength of the dominant response spikes stays practically constant. In parallel, the diffusive response becomes pronounced more and more. Closest to the SN bifurcation, an optical power as low as 100 fJ is sufficient for excitation. The calculation verifies that the threshold is determined by the saddle-node separation (fig. 6a), in full agreement with the role of the stable saddle-manifold as separatrix. Various facts clearly signify that the excitable dynamics of the system close to the boundary crisis is correlated with the former CA. First, the experimental spike heights agree very well with the maximum output fluctuations of the device for $I_P < I_c$ (fig. 6b) and no injection. Second, the power spectrum under optical stimulation is practically identical with that in the chaotic regime (fig. 2b). Third, as will be detailed in the remainder, the transient spike trains subsequent to stimulation are highly irregular in frequency and amplitude.

Figure 7 summarizes calculated and experimentally detected response transients close to the boundary crisis. The cw state prior to excitation is characterized by a power as well as an optical phase. The latter is random in the measurements because of a phase drift between successive excitation steps due to unavoidable experimental noise. The two transients in fig. 7a are computed for the same stimulus strength but slightly different initial phases. The spike trains coincide only initially but diverge after longer times. One transient (grey) approaches equilibrium already after 3 ns, while the other one (black) keeps spiking as long as 20 ns. Such extreme sensitivity on the initial conditions is a clear fingerprint of chaotic dynamics associated with the motion along the CS. Indeed, also in the calculations, the excited spike sequences resemble very well the power fluctuations in the CA just before the boundary crisis. Furthermore, as can be tracked in the numerics, the irregular spiking always stops when the trajectory passes the separatrix close to the saddle-focus.

The sampling technique used experimentally provides one data point per stimulation event in the power-time diagram. Repeating the time scans sufficiently often yields

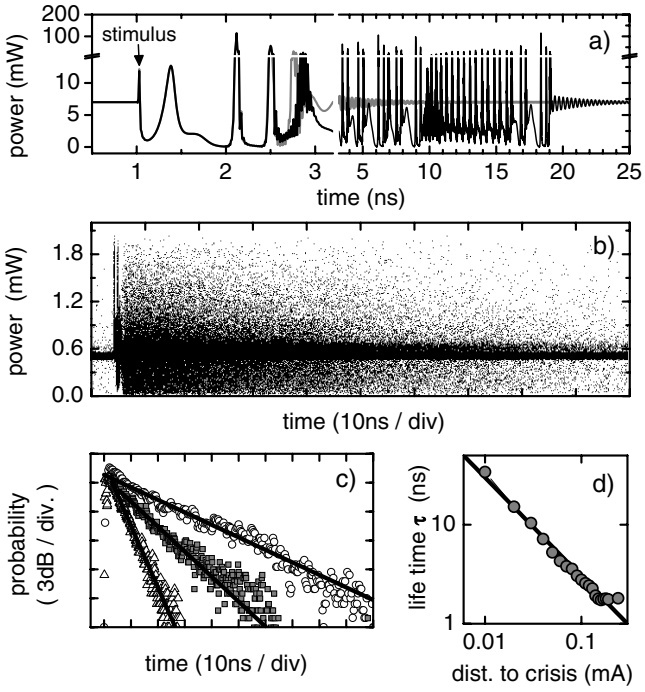

Fig. 7: Excitable chaotic transients. a) Calculated response at $\phi = 4.15$ and a stimulus of 1 pJ. The two cases differ only by the initial optical phase of the rest state. b) Experimental response at $I_P - I_c = 0.01\,\mathrm{mA}$. The plot is a superposition of 500 repetitive scans with 500 data points each. c) Probability of presence in the CS *vs.* time after stimulation for three different distances from the boundary crisis $I_P - I_c$: 0.04 mA (triangles), 0.02 mA (squares), and 0.01 mA (circles). Lines: singe-exponential fits. d) Mean lifetime τ on the CS *vs.* $I_P - I_c$. Solid line: inverse-power function with exponent $\gamma = 1$.

then the probability that the device emits a certain power at given time. An example of such measurement is displayed in fig. 7b. Chaotic transients differ from each other after a time of the order of the largest inverse Lyapunov exponent. Consistently, a pair of quasi-deterministic spikes is seen at very early times in fig. 5b. Later spikes are irregularly spaced and yield thus only a cloud of uncorrelated dots. The latter starts few nanoseconds after stimulation, which is in fair agreement with the numerically calculated Lyapunov exponents. The power distribution along a vertical line in fig. 7b is a superposition of the narrow Gaussian related to the rest state and a much broader band due to the chaotic response. The area below the wide band is a measure for the probability to find the system still in the CS at this time. Extracting this area from the data and plotting it versus time (fig. 7c) reveal that this probability decays strictly single-exponential with a time constant τ representing the mean lifetime in the CS. This lifetime becomes shorter with increasing distance from the boundary crisis. As long as the distance is not too large, τ obeys an inverse-power law $\sim (I_P - I_c)^{-\gamma}$ with a critical exponent $\gamma \approx 1$ (fig. 7d). Beyond $I_P - I_c \approx 0.1\,\mathrm{mA}$,

[1]The rotational invariance of the optical equations is not accounted here. It gives another zero Lyapunov exponent and increases the attractor dimension by one.

saturation sets on and τ approaches a constant value of about 1.8 ns. In parallel, as already noted above, the response of the device becomes increasingly dominated by a single spike and is thus fully analogous to the previously observed excitability at a homoclinic bifurcation [14].

A time-independent escape rate $1/\tau$ from the CS is a generic property of chaotic transients [19–21]. Inverse-power laws are well established for one- or two-dimensional maps [19] and have been experimentally verified in a nonautonomous mechanical system [20]. Three dimensions have been treated theoretically only very recently [21]. The present study provides direct evidence that an inverse-power law remains valid also for the boundary crisis of a high-dimensional CA in a continuous and autonomous system. The critical exponent of one-dimensional maps is generically 0.5 [19], a three-dimensional example has yielded 1.5 [21], and those of two-dimensional maps lie in between. It has been argued [19] that the critical exponents should increase with the dimension of the chaos. Our results do not confirm this conjecture: In the continuous system under study, γ is close to 1 although the estimated dimension of the CA is as large as 3.5.

Noise in the presence of a CS can also induce chaotic behavior [22]. In order to investigate the role of noise in the multi-section laser, we have repeated the measurements without external excitation. Indeed, close to the boundary crisis, random jumps into chaotic transients are observed. However, in marked contrast to the excitable dynamics, their probability decreases very rapidly with the distance from the crisis and becomes negligible already at an excess current of 0.01 mA. Noise-induced dynamics is thus of minor importance in our case. In particular, the few data points in fig. 7b before application of the excitation pulse are not a result of noise but correspond to chaotic transients which last longer than the 200 ns separation between subsequent stimuli. Such an extremely extended response is a characteristic feature of a CS: It involves trajectories wandering arbitrarily long in the saddle before approaching an attractor.

In conclusion, using a semiconductor laser device, excitability of high-dimensional chaotic transients has been observed in a continuous and autonomous system. The escape from the underlying CS is strictly single-exponential and validity of an inverse-power law for the escape time is found close to the boundary crisis. Despite the high dimensionality, the critical exponent is close to unity. The excitation of the chaotic transient exhibits a distinct threshold as well as a refractory time and, sufficiently far from the boundary crisis, the standard response of excitable systems is recovered. The relaxation times of the carrier-photon dynamics in the laser are in the sub-ns range. A striking finding from a practical point of view is therefore that the device is capable of emitting pulses with a delay on a two orders of magnitude longer time scale. This might have a number of application, *e.g.*, in the emerging field of chaos communication or in networks of lasers with excitable chaos.

* * *

This work was supported by Deutsche Forschungsgemeinschaft within Sfb 555 and by the research center Matheon. The authors thank Bernd Sartorius, Fraunhofer-HHI Berlin, for providing the laser device. We also acknowledge assistance of Stefan Bauer and contributions made by Alexander Betke in his diploma thesis [23].

REFERENCES

[1] Hodgkin A. L., *J. Physiol.*, **107** (1948) 165.
[2] Murray J. D., *Mathematical Biology* (Springer, New York) 1990.
[3] Clother D. R. and Brindley J., *J. Math. Biol.*, **39** (1999) 377.
[4] Zhabotinsky A. and Zaikin A., *Nature (London)*, **225** (1970) 535.
[5] Tredicce J. R., in *Fundamental Issues of Nonlinear Laser Dynamics*, edited by Krauskopf B. and Lenstra D., *AIP Conf. Proc.*, Vol. **548** (AIP Melville, New York) (2000) p. 238.
[6] Krauskopf B. *et al.*, *Opt. Commun.*, **215** (2003) 367.
[7] Giudici *et al.*, *Phys. Rev. E*, **55** (1997) 6414.
[8] Grebogi C., Ott E. and Yorke J. A., *Phys. Rev. Lett.*, **48** (1982) 1507; *Physica D*, **7** (1983) 181.
[9] Papoff F., Dangoisse D., Poite-Hanoteau E. and Glorieux P., *Opt. Commun.*, **67** (1988) 358.
[10] Meucci R. *et al.*, *Phys. Rev. Lett.*, **95** (2005) 184101.
[11] Jánosi I. M., Flepp L. and Tél T., *Phys. Rev. Lett.*, **73** (1994) 529.
[12] Wieczorek S., Krauskopf B. and Lenstra D., *Phys. Rev. E*, **64** (2001) 056204.
[13] Izhikevich E. M., *Int. J. Bifurcation Chaos*, **10** (2000) 1171.
[14] Wünsche H.-J. *et al.*, *Phys. Rev. Lett.*, **88** (2002) 023901.
[15] Plaza F. *et al.*, *Europhys. Lett.*, **38** (1997) 85.
[16] Bauer S. *et al.*, *Phys. Rev. E*, **69** (2004) 016206; Ushakov O. *et al.*, *Phys. Rev. Lett.*, **92** (2004) 043902.
[17] Radziunas M., *Physica D*, **213** (2006) 98.
[18] Wolf A. *et al.*, *Physica D*, **16** (1985) 285.
[19] Grebogi C., Ott E. and Yorke J. A., *Phys. Rev. Lett.*, **57** (1986) 1284; Grebogi C., Ott E., Romeiras F. and Yorke J. A., *Phys. Rev. A*, **36** (1987) 5365.
[20] Ditto W. L. *et al.*, *Phys. Rev. Lett.*, **63** (1989) 923; Sommerer J. C. *et al.*, *Phys. Lett. A*, **153** (1991) 105.
[21] Alligood K. T., Sander E. and Yorke J. A., *Phys. Rev. Lett.*, **96** (2006) 244103.
[22] Lai Y.-C. *et al.*, *Phys. Rev. E*, **67** (2003) 026210.
[23] Betke A., *Erregbarkeit in Mehsektions-Halbleiterlasern*, Diplomarbeit, Mathematisch-Naturwissenschaftliche Fakultät der Humboldt-Universität zu Berlin, 2003.